Abstract

In the baseline Neutrino Factory muon front end, intense, highly packed solenoidal fields are used to contain the high emittance muon beam. In addition, significant acceleration is required for bunching, phase rotation and cooling, requiring RF cavities operating near to their maximum achievable gradient. There are experimental indications that RF cavities cannot achieve these large gradients in the presence of such intense magnetic fields. In this paper, I discuss the design of a muon cooling channel that is designed with RF cavities removed from the intense magnetic fields, and examine the change in performance that results from this compromise.

High Acceptance Muon Ionisation Cooling Channel with Magnetically Shielded RF Cavities

October 9, 2012

1 Cooling for the Neutrino Factory

In the Neutrino Factory [1], protons are fired onto a target to produce pions. The pions are captured in a 20 T solenoidal field which is tapered to a 1-2 T constant field. Pions and their decay products, the muons, are allowed to drift longitudinally in a constant field solenoid and subsequently a variable frequency RF system is used to bunch and then phase rotate the muons. Muons are then passed through an alternating solenoid lattice where the beam is cooled in transverse phase space by means of ionisation cooling. Then the beam is accelerated in a sequence of linacs, recirculators and a Fixed Field Alternating Gradient ring. The muons are then passed into a storage ring where the muons decay to neutrinos.

Despite the phase rotation system, the beam has a large phase space upon entry to the cooling section. The distribution in transverse amplitude and momentum for a typical beam is shown in Figure **??**.

1.1 Ionisation Cooling

In this paper a new design for the ionisation cooling part of the accelerator chain is studied. In ionisation cooling, particles are passed through an absorber where their energy is reduced. Subsequently the particles are reaccelerated in only the longitudinal direction resulting in an overall reduction

in transverse emittance. Stochastic effects such as multiple Coulomb scattering tend to reduce the amount of cooling achieved or even heat the beam. The change in transverse beam emittance ϵ_n for a cylindrically symmetric beam with beam particles with energy E and mass m on passing through a thin absorber of thickness dz can be written as [**?**]

$$\frac{d\epsilon_n}{dz} \approx \frac{1}{\beta_{rel}^2 E}\left\langle\frac{dE}{dz}\right\rangle\epsilon_n + \frac{1}{2m}\frac{13.6^2}{L_R}\frac{\beta_\perp}{\beta_{rel}^3 E}. \quad (1)$$

Here β_{rel} is the particle velocity normalised to the speed of light, $beta_\perp$ is the transverse β function and L_R is the radiation length of the material. The left hand term is the cooling term due to energy loss while the right hand term is a heating term due to multiple scattering. The emittance at equilibrium can be found by setting $d\epsilon_n/dz$ to 0 so that

$$\epsilon_n(equilibrium) = \frac{1}{2m}\frac{13.6^2}{L_R}\frac{\beta_\perp}{\beta_{rel} < \frac{dE}{dz} >}. \quad (2)$$

Below this emittance, the beam will be heated more by multiple scattering effects than it will be cooled by energy reduction. The equilibrium emittance for a few different materials is shown in Figure 1.

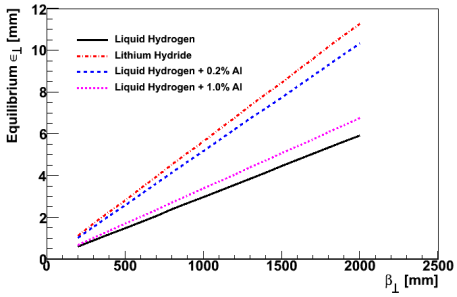

Figure 1: Equilibrium emittance as a function of transverse β function for various materials.

1.2 RF Problem

In the Neutrino Factory baseline front end design, RF cavities are planned to operate near to the Kilpatrik limit despite the presence of magnetic fields

around 2 T. There is some evidence that the presence of these strong fields may limit the RF cavity peak field by a factor of roughly 2, although experiments have been limited by a number of factors and further work is needed [2]. Several schemes have been investigated to work around this problem. Magnetically insulated RF cavities have been considered, whereby the magnetic field is configured to be orthogonal to the surface in the hope that this may improve the peak field that can be achieved by the RF [3]; and RF cavities have been considered with high pressure gas that acts as an insulator to the cavity [4].

1.3 Shielded RF cavities

In this paper the possibility of modifying the design of the cooling channel so that the RF cavities no longer sit in intense magnetic fields is studied. This is advantageous over other schemes as the technical risk associated with the design is reduced and no additional hardware research and development is required. In addition, the designs presented are rather less aggressive than the baseline and may be easier to construct and operate. In order to extract the RF cavities from the magnetic fields, the cell is lengthened and shielding is placed around the coils to reduce stray fields. As will be shown, the presence of shielding reduces the transverse acceptance of the lattice resulting in a poorer performance.

Schematics of the cooling arrangements considered in this paper are shown in Figure 2. Three arrangements are considered, each with equally spaced superconducting magnets, normal conducting RF cavities and liquid Hydrogen absorbers.

In the Neutrino Factory front-end, the cooling performance is limited by two factors: the equilibrium emittance of the cooling system that is a function of the material used for cooling and the amount of focussing on the absorber; and the acceptance of the cooling channel, the maximum beam emittance of the beam that can be passed into the cooling channel, a function of non-linear terms in the beam optics.

2 Solenoidal Lattice

The theory of linear and non-linear beam transport through solenoids has been well-established. It is possible to relate the Hamiltonian for a solenoid to

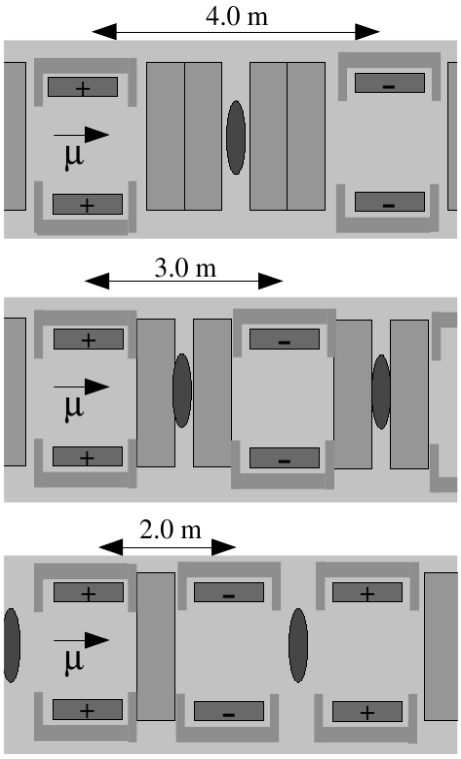

Figure 2: Schematic of the three different lattices that I consider in this paper. Coils are shown marked with a '+' or '-' to indicate polarity, absorbers are shown as dark grey ellipses while RF cavities are shown as light grey rectangles. With the additional shielding discussed below, cavities sit in fields ¡ 0.2 T.

the properties of the beam transport such as focussing power and acceptance.

2.1 Equations of Motion in a Solenoid

The Hamiltonian for a solenoid can be written as a power law[?]

$$H(\vec{u}^c; z) = H_0 + H_1 + H_2 + \dots \tag{3}$$

where H_i describes a polynomial expanded about the reference trajectory in the canonical phase space vector $\vec{u}^c = (x, y, t, p_x^c, p_y^c, p_t^c)$ of order i and

$$\begin{aligned}
K_0 &= \frac{p_0}{v_0}(1 + v_0^2) && (4)\\
K_1 &= 0 && (5)\\
K_2 &= \frac{(p_x^c)^2 + (p_y^c)^2}{2p} - \frac{B_0}{2p}(xp_y^c - yp_x^c) + \frac{B_0^2}{8p}(x^2 + y^2) \\
&\quad + \frac{(p_t^c)^2}{2p\beta_{rel}^2\gamma_{rel}^2} && (6)\\
K_3 &= p_t^c K_2/\beta_{rel} && (7)\\
K_4 &= SOMETHINGHERE && (8)\\
K_5 &= \dots && (9)\\
& && (10)
\end{aligned}$$

In a magnetic field, momentum is conserved. To calculate the transverse acceptance at a given energy, the energy coordinate can be set to the reference energy such that $p_c^t = 0$ for all particles and

$$\begin{aligned}
eq : hamiltonian) K_0 &= \frac{p_0}{v_0}(1 + v_0^2) && (11)\\
K_1 &= 0 && (12)\\
K_2 &= \frac{(p_x^c)^2 + (p_y^c)^2}{2p} - \frac{B_0}{2p}(xp_y^c - yp_x^c) + \frac{B_0^2}{8p}(x^2 + y^2) && (13)\\
K_3 &= 0 && (14)\\
K_4 &= SOMETHINGHERE && (15)\\
K_5 &= \dots && (16)\\
& && (17)
\end{aligned}$$

The polynomial mapping from $\vec{u}(z) \rightarrow \vec{u}(z+dz)$ can be found using the Poisson bracket operation,

$$\frac{d\vec{u}}{dz} = -[K, \vec{u}^c] = -\frac{\partial K}{\partial q_i}\frac{\partial u}{\partial p_i} + \frac{\partial K}{\partial p_i}\frac{\partial u}{\partial q_i}. \tag{18}$$

2.2 Transverse Focussing

In order to keep the RF cavities out of the strongest magnetic fields it is necessary to make a lattice with a length of a few metres. The peak field of the 800 MHz cavity shown in Figure **??** is reduced by about 40 % even at fields as low as 0.6 T, while it is apparently unaffected below about 0.2 T. In order to decouple the cavity performance from the magnetic field strength, the lattice in this paper is designed with the aim of keeping magnetic fields well below 0.5 T. This necessitates a cell with a length of several metres.

The transverse Twiss parameter $\beta_\perp$ at 230 MeV/c is shown as a function of position in the cell and momentum for cells with coils separated by 0.75, 2, 3 and 4 metres. In each case the strength of the solenoids has been adjusted to ensure $\beta_\perp$ is at 1200 mm on the absorber, sufficient to give an equilibrium emittance of order 6 mm in liquid Hydrogen. $\beta_\perp$ goes to 0 for lower momenta due to the linear resonance in this region. Although the Twiss parameter at the central momentum can be maintained at an arbitrary value, as the lattice length is increased, the momentum acceptance is reduced. Stretching the lattice can be used to remove RF cavities from the magnetic fields, but only at the expense of less focussing at the absorber of a smaller momentum acceptance.

An alternative method to remove the RF cavities from the magnetic fields would be to introduce shielding around the solenoids in order to shorten the fringe field. The focussing power of the solenoids goes as $\int B_z^2 dz$ so the fringe fields do not contribute much to the focussing.

2.3 Solenoid Lattice Acceptance

It is somewhat intuitive that lattices with lower radius coils have a lower acceptance. Particles that travel near to the coils see a region of poor field quality and this leads to emittance growth and beam loss of high amplitude particles. However, the Hamiltonian for a solenoidal field is expressed purely in terms of the on-axis field so that the beam dynamics is uniquely described

by this on-axis field and so there is conceptually no difference between a coil of low radius and a coil with a very short fringe field.

The linear terms in the Hamiltonian describe the emittance conserving transverse focussing of the lattice while non-linear terms can cause emittance growth [**?**]. Examining the expression for K_4 in **??**, it can be seen that there are terms that relate to B_0

2.4 Effect of Absorbers and RF cavities

The introduction of cooling hardware introduces a cell-by-cell energy change into the lattice. The Hamiltonian for a superimposed RF and solenoid can be written as

$$
\begin{aligned}
K_0 &= SOMETHINGHERE && (19)\\
K_1 &= 0 && (20)\\
K_2 &= \frac{(p_x^c)^2 + (p_y^c)^2}{2p} - \frac{B_0}{2p}(xp_y^c - yp_x^c) + \frac{B_0^2}{8p}(x^2 + y^2) && (21)\\
K_3 &= 0 && (22)\\
K_4 &= SOMETHINGHERE && (23)\\
K_5 &= \ldots && (24)\\
& && (25)
\end{aligned}
$$

There is now a coupling between transverse and longitudinal phase space. In the lattices considered here, the longitudinal phase advance is small and the focussing due to the RF cavity is also small so that the coupling between longitudinal and transverse phase spaces is weak.

2.5 Focussing Power

In order to achieve good performance, it is necessary to develop a lattice with tight focussing on the absorbers. A tightly focussed beam necessarily has a large transverse momentum, which offers two advantages; the transverse momentum loss is greater compared to the longitudinal momentum leading to greater cooling; and the effect of multiple scattering is less as a proportion of the total transverse momentum. This can be summarised in a parameter, the equilibrium emittance, that describes the transverse beam emittance where the ionisation cooling effect is in equilibrium with the mutliple scattering heating effect. The equilibrium emittance as a function of optical β

function is shown in Figure **??** for various different materials. Lengthening the cell makes it harder to achieve low β functions, so that in this note I will only consider liquid Hydrogen absorbers. These absorbers are challenging to construct and may make maintenance and operation of the beam cooling system more demanding.

Achieving tight focussing over a broad range of momenta, as we have in the Neutrino Factory front end, is a challenging proposition. In Figure 3 the length of the cooling cell is increased and the transverse β function is examined at the focus as a function of momentum. Here the lattice was made up of identical solenoids with 2.5 m separation, with adjacent coils having opposite polarity. It can be seen that increasing the cell length also increases $d\beta/dp$, thus limiting the momentum range over which longer-celled cooling channels can operate.

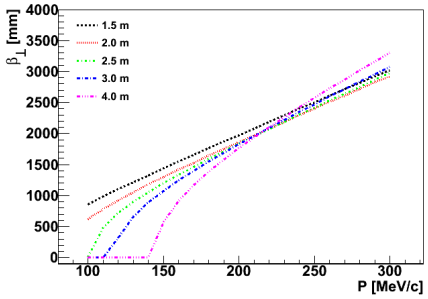

Figure 3: Transverse β function at the focal point, equidistant between coils, as a function of momentum for lattices with various coil separations.

2.6 Transverse Acceptance

Another challenge in the design of these shielded-RF cooling channels is maintaining a large transverse acceptance. The transverse acceptance for lattices with coils of various radii is shown in Figure 4 for a typical cooling cell. Here the transverse acceptance is calculated by tracking a few muons of a certain amplitude through 20 cells of the accelerator. Those muons that gain more than 25% in transverse amplitude are considered outside the acceptance of the cooling channel.

It is clear that coils with lower radius lead to a channel with smaller acceptance. This is somewhat intuitive. However, the field of a solenoidal

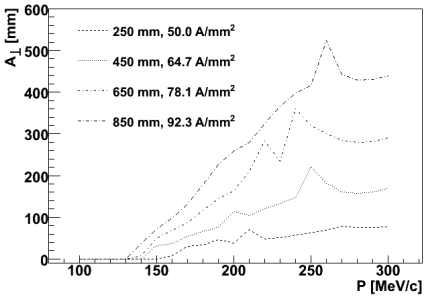

Figure 4: Acceptance for a variety of coils of various radius. $< B_z^2 >$ is fixed so that the focussing power of the coils is the same in each case.

focussing system is dependent only on the on-axis field and so the optics of the focussing system is also dependent only on the on-axis field. The effect of lowering the radius of the coils is to shorten the end field of the coil and this leads to a strong non-linear component to the focussing field.

The term for $n = 0$ gives linear focussing terms. The dependence of linear focussing on momentum gives a second order chromatic aberration term, effectively the variation of β with momentum shown in Figure 3. Both the $n = 0$ and $n = 2$ terms contribute a spherical aberration at third order.

One might expect then that in the presence of fields that are tapered quickly, for example due to a lower radius or the presence of shielding, d^2B_z/dz is large, spherical aberrations are strong and the transverse acceptance is limited. I have tracked an ensemble of particles through solenoidal field maps using the power-law expansion in (**??**) together with a '*tanh*' field on-axis, given by

$$B_z(r = 0, z) = \frac{B_0}{2}\left[\tanh\left(\frac{z - z_0}{\lambda}\right) + \tanh\left(\frac{z_0 - z}{\lambda}\right)\right], \tag{26}$$

where λ is the end length and z_0 is the centre length. The mapping of particles from the beginning of a cell to the end of a cell was then calculated using a linear-least-squares fit of particle trajectories between the cell beginning and end, under the additional constraint that higher amplitude particles were removed from the fit until the fitted data matched the tracking data. The algorithm was observed to be stable for several different ensembles of particles and for a range of step sizes in the numerical tracking.

The strength of the various third order coefficients is shown for a number of different end-field lengths λ in Figure 5, while keeping the paraxial

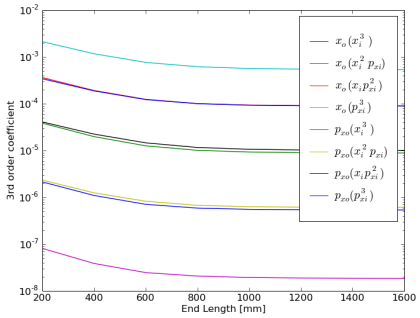

Figure 5: Some third order terms in the polynomial mapping through a cell with 2.5 m coil spacing, as a function of end length, for a tanh field model with 800 mm centre length.

focussing strength, given by $\int B_z^2(r=0)dz$, constant. It can be seen that as the field is more quickly tapered, the non-linear terms are considerably stronger.

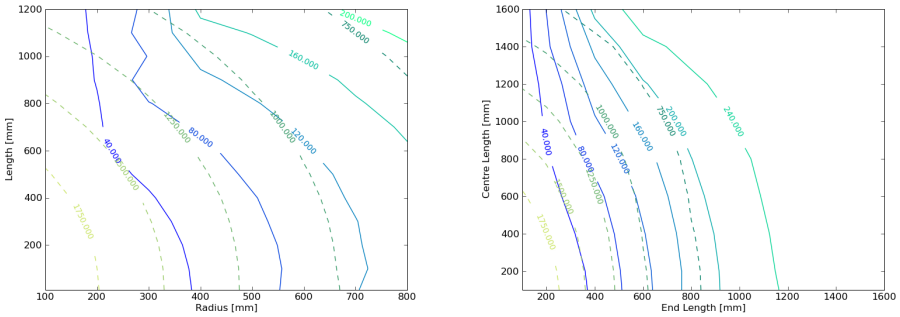

Figure 6: Acceptance as a function of (full) coil parameters and (dashed) length of the field-free ($B_z < 0.5T$) region in a 2.5 m lattice. The field is calculated both (left) for a tanh field model and (right) for a multiple-sheet model of the coils.

The effect of these non-linear terms on transverse acceptance is shown in Figure 6 both for a coil simulated using the *tanh* model outlined above and for a coil simulated using a sheet model. In the first instance both the end length λ and central field length z_0 were changed, while in the second instance the coil radius and length were changed. The radial thickness of

the coil was maintained at 100 mm. In addition, the length of the field-free region is shown, taken as the region with $B_z < 0.5T$, for a lattice with a length of 2.5 m.

3 Lattice Length

In light of these constraints, I consider three different lattices, with a distance of 2, 3 and 4 metres between coils. The shorter lattices have better quality lattice optics but worse RF packing fractions. Schematic diagrams of each lattice is shown in Figure 2. The transverse β function for different lattices is shown in Figure 3. For the same β function the momentum acceptance decreases as the lattice length is increased.

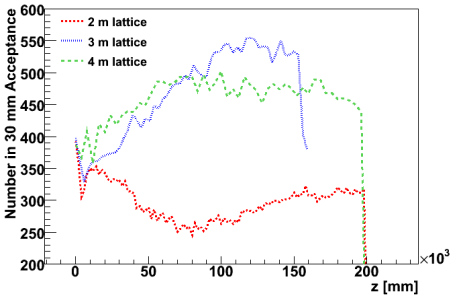

Figure 7: Increase in number of muons in a nominal accelerator acceptance of 30 mm transverse and 100-300 MeV/c momentum, for the different cell lengths.

A beam was tracked through each of the accelerator lattices and the results are shown in Figure 7. Here the increase in the number of muons in an acceptance of 30 mm is shown for a beam of particles tracked through the baseline front end up to the end of the phase rotation section. A transverse matching was assumed by taking a single, emittance conserving linear transformation to the transverse β function of each lattice. It is clear that the 3 m lattice shows the best performance. However, there appears to be an initial transverse mismatch in all cases that leads to some beam heating at the start of the cooling section. It is noted that the longer cell performs better initially, indicating that there may be a slight optimisation to switch between the two cases.

4 Momentum Dependence

¡Cooling performance as a function of momentum dependence !!!¿

¡Cooling performance as a function of length and momentum dependence? !!!¿

5 Coil Models and Shielding

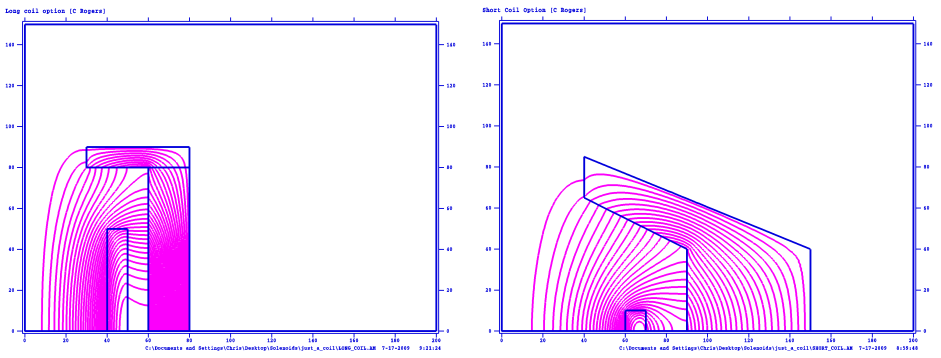

Figure 8: (left) Long coil and (right) short coil options for the lattice.

I have performed some initial studies to understand what coil geometries are desirable and how much the end field of the coils can be tapered. In the first instance I have studied the use of iron as a shielding material, although it may be profitable to use a bucking coil arrangement in addition to iron shielding. As noted above, strong shielding has an adverse effect on beam optics and should be avoided.

In Figure 8 I show two coil designs, both chosen to have a transverse acceptance of about 100 mm. The first design is longer with a lower radius while the second design is shorter with a larger radius. The options were chosen to have a similar compromise between acceptance and field-free region length. The short coil design has a 0.109 m^3 of superconductor but 100 A/mm^2 current densities. The long coil design has 0.377 m^3 of superconductor and 18 A/mm^2 current density. The total volume of iron shielding for the latter case is considerably smaller.

In both cases I have used iron to provide shielding of the RF cavities from the fringe field of the magnet. This enables the maximum magnetic field on the RF cavity to be reduced from 0.5 T to 0.1 T. In addition it may have

practical advantages; stray fields will not effect hardware near to the cooling channel and stray iron near to the accelerator will not steer the beam. It may be desirable to use bucking coils to provide the main shielding, with additional iron shielding any remaining stray fields.

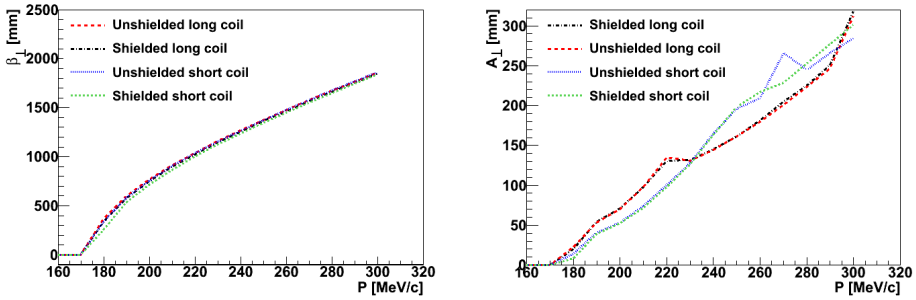

Figure 9: (left) Transverse β function and (right) transverse acceptance for the coils, with a 3 m distance between coils.

I have shielded only the edge of the field, so that the optics is unaffected by the shielding. The transverse beta function and acceptance of the lattice for the two coils, with and without shielding, is shown in Figure 9. With an appropriate scaling of fields, there is practically no difference in the optics.

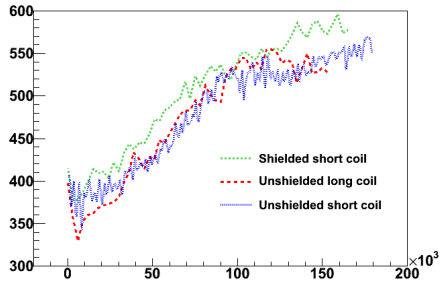

Figure 10: Change in number of muons within a 30 mm transverse acceptance for the long and short coil options.

The cooling performance is shown in Figure 10. The long coil option performs slightly worse, although there is a noticeable drop in muon efficiency at input to the channel that probably indicates an initial mismatch indicating that with more attention to matching it may be possible to do better.

6 Full Lattice

¡Full lattice including acceleration sections and so on!!!¿.

7 Doublet and Triplet Lattice

¡Investigate doublet and triplet lattices!!!¿

8 Conclusions

I have presented a study of the use of a simple two coil lattice for the cooling section of the muon front end of the Neutrino Factory, under the constraint that the RF cavities should sit in relatively low magnetic fields. I have studied the momentum acceptance and transverse acceptance of the lattice as a function of the fringe field length of the coils to understand how much shielding can be used, and I have examined two different designs for coils including some small shielding of the fringe. Overall, I have been able to design a cooling channel with performance worse than, but comparable to, the IDS baseline. Studies continue.

References

[1] Accelerator design concept for future neutrino facilities (ISS), Journal of Instrumentation, Volume 07, Issue 07, pp. 07001 (2009).

[2] A. Moretti et al., Effects of high solenoidal magnetic elds on rf accelerating cavities, PRSTAB 8, 072001, 2005.

[3] R. Palmer et al., RF Breakdown with and without External Magnetic Fields, PRSTAB 12, 031002, 2009.

[4] P. Hanlet et al., High Pressure RF Cavities in Magnetic Fields, Proc. EPAC 2006, 2006.

[5] A.J. Dragt, Numerical Third-Order Transfer Map for Solenoid, NIM A 298, 441-459, 1990.

[6] A.B. El-Kareh and J.C.El-Kareh, Electron Beams, Lenses and Optics 2, 20, 1970.